JOURNAL OF PHYSICAL ORGANIC CHEMISTRY
J. Phys. Org. Chem. 2000; **13:** 395–404

Solid-state study of cyclic thiohydroxamic acids: 1-hydroxy-2(1*H*)-pyridinethione and 3-hydroxy-4-methyl-2(3*H*)-thiazolethione

Andrew D. Bond and William Jones*

Department of Chemistry, University of Cambridge, Lensfield Road, Cambridge, CB2 1EW, UK

Received 14 February 2000; revised 28 March 2000; accepted 3 April 2000

epoc

ABSTRACT: Cyclic thiohydroxamic acids such as 1-hydroxy-2(1*H*)-pyridinethione (1) and 3-hydroxy-4-methyl-2(3*H*)-thiazolethione (2) find diverse applications as fungicides and alkoxy-radical precursors. Selected physico-chemical properties such as thermal stability can be rationalized by examination of their solid-state structures. We report here a new hydrated form of 2 (denoted 3) that displays enhanced thermal stability and solubility compared with the anhydrous form. These enhanced properties may be attributed to the ionic nature of 3 in the solid state. The oxidized form of 1, 2,2′-dithiobis(pyridine-1-oxide) (DTPO, 4) also finds application as a fungicide. Attempts to produce an analogous disulfide from 2 produced a new thioether product, 3-hydroxy-4-{[3-oxo-4-methyl-2(3*H*)-thiazol-2-yl]thio}-2(3*H*)-thiazolethione (5). Co-crystallization of 1 with 2 produced a mixed molecular crystal (6) containing both DTPO and a new thioether derivative of 2, 5,5′-thiobis[3-hydroxy-4-methyl-2(3*H*)-thiazolethione]. The supramolecular complementarity of the two components gives rise to discrete hydrogen-bonded dimers within the co-crystal. Copyright © 2000 John Wiley & Sons, Ltd.
Additional material for this paper is available from the epoc website at http://www.wiley.com/epoc

KEYWORDS: thiohydroxamic acids; solid-state structure; molecular crystals; hydrates; co-crystals; supramolecular chemistry; host–guest complexes; physico-chemical properties

INTRODUCTION

The solid-state structure adopted by an organic material can have a profound influence upon its physico-chemical properties and reactivity.[1] A given molecular component in various solid-state arrangements (i.e. within different polymorphic forms) may exhibit different properties including thermal stability, equilibrium solubility and dissolution rate (for a review of polymorphism in molecular crystals and its thermodynamic and structural implications, see Ref. 2). Such differences can be of vital importance. In the pharmaceutical industry, for example, the inadvertent production of an unexpected polymorph or hydrate may lead to the administration of ineffective or toxic dosages.[3] Consideration of solid-state structure in addition to molecular structure is, therefore, essential. As knowledge of the relationship between solid-state structure and reactivity develops for a particular material, the possibility arises of tailoring the structure for applications where specific properties are necessary. As a result, the modification of the solid-state structure of materials in a controlled manner may, in general, allow for the production of structural variants with enhanced properties. Strategies which are adopted for structure modification include the production of new polymorphs, solvates and mixed molecular crystals.[4,5]

We are currently studying the solid-state chemistry of cyclic thiohydroxamic acids, which find application in two diverse areas. First, materials based on pyridinethiones, such as 1-hydroxy-2(1*H*)-pyridinethione (pyrithione, **1**), are widely used as fungicides.[6] It has been suggested that the effectiveness of pyrithione as a fungicide is predominantly based upon chelation complex formation.[7] Although less extensively studied, 3-hydroxy-4-methyl-2(3*H*)-thiazolethione (HMTT, **2**) has a chelating unit similar to that of pyrithione and might therefore be expected to exhibit similar antimicrobial activity. *O*-Esters of pyrithione have also been used as alkoxy-radical precursors in synthetic procedures and mechanistic studies.[8] Their convenient application in synthesis is hindered, however, by significant sensitivity to light, resulting in short shelf-lives for such reagents. It has been suggested that *O*-esters based upon 2(3*H*)-thiazolethione derivatives offer improved stability compared with those based upon pyridinethiones.[9] A procedure for the selective *O*-alkylation of 2(3*H*)-thiazolethiones has recently been reported, and such

**Correspondence to:* W. Jones, Department of Chemistry, University of Cambridge, Lensfield Road, Cambridge CB2 1EW, UK.
E-mail: wj10@cam.ac.uk
Contract/grant sponsor: EPSRC.

derivatives have been employed successfully as sources of oxygen-centred radicals.[10]

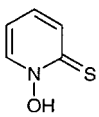

pyrithione (1)

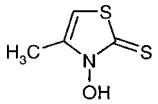

HMTT (2)

The crystal structures of **1** and **2** have been determined previously[10,11] (A. D. Bond, N. Feeder, S. J. Teat and W. Jones, Tetrahedron submitted for publication). In this paper, the structures are re-examined from the perspective of their relationship with selected physico-chemical properties of the materials. Additionally, several avenues for structure modification have been explored. A hydrated phase of **2** (denoted **3**) which displays properties markedly different from those of the anhydrous material is reported here. The oxidized derivative of **1**, 2,2′-dithiobis(pyridine-1-oxide) (DTPO, **4**) also finds application as a fungicide[6] and has been shown to have a solid-state structure suitable for guest inclusion.[12,13] In an attempt to prepare from **2** a disulfide analogous to DTPO, we have prepared a thioether product, 3-hydroxy-4-{[3-oxo-4-methyl-2(3*H*)-thiazol-2-yl]thio}-2(3*H*)-thiazolethione (**5**) and determined its crystal structure. Finally, by co-crystallization of **1** and **2**, we have produced a new mixed molecular material (**6**), containing both DTPO and a new thioether derivative of **2**, 5,5′-thiobis[3-hydroxy-4-methyl-2(3*H*)-thiazolethione].

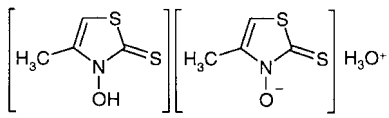

3

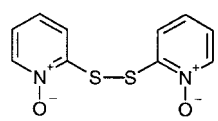

DTPO (4)

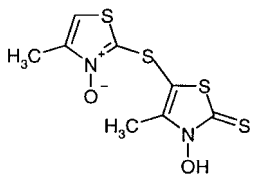

5

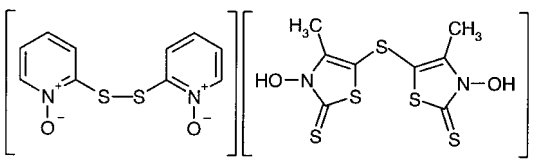

[DTPO][THMTT] (6)

RESULTS

Crystal structure of the hydrate 3

The hydrate **3** contains two independent HMTT moieties

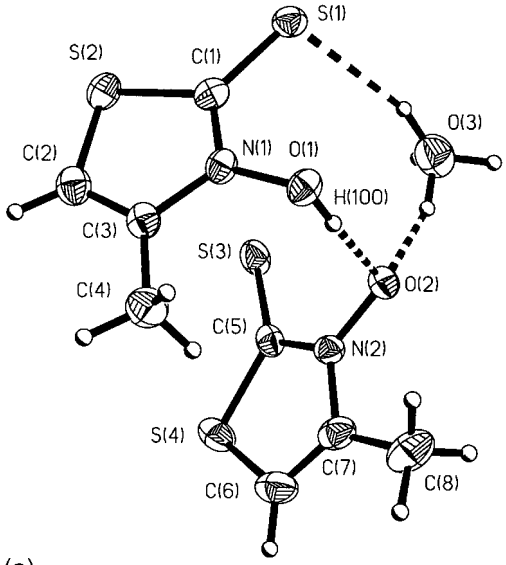

(a)

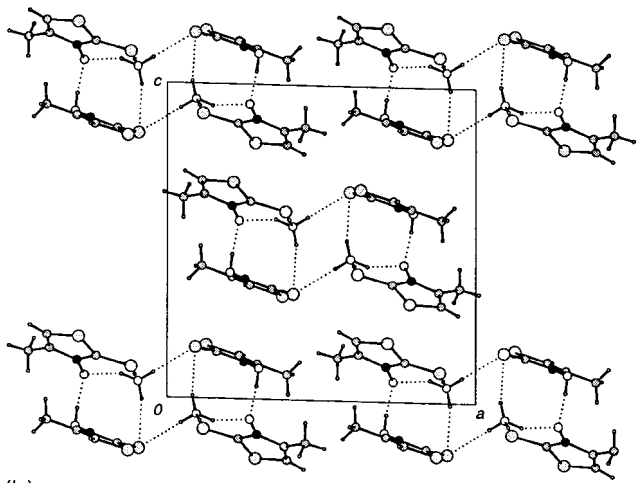

(b)

Figure 1. (a) Asymmetric unit of the hydrate **3** showing displacement ellipsoids at 50% probability. Hydrogen-bond interactions are indicated by dotted lines. (b) View of **3** along the *b* direction, showing the molecules linked via O—H···O and O—H···S interactions into 'double chains' running out of the plane of the page

in the asymmetric unit, together with a water molecule [Fig. 1(a)]. The possibility of thiol–thione tautomerism exists in solution for the HMTT molecule and the anhydrous material **2** has been shown to exist as the thione in the solid state (A. D. Bond, N. Feeder, S. J. Teat and W. Jones, Tetrahedron submitted for publication). In one of the HMTT moieties in **3**, the C(1)—S(1) and N(1)—O(1) bond distances are comparable to those in **2** (Table 1). The location of H(100) in a difference Fourier map confirms that the first HMTT moiety is present as the thione tautomer. The C(5)—S(3) and N(2)—O(2) bond distances of the second HMTT moiety are not significantly different (Table 1), but no hydrogen atom could be

Table 1. Selected C—S and N—O bond distances for **3, 5** and **6**

Compound	Bond	Distance (Å)	Assignment
3	C(1)—S(1)	1.695(4)	C=S
	C(5)—S(3)	1.685(4)	C=S
	N(1)—O(1)	1.368(4)	N—O(H)
	N(2)—O(2)	1.357(4)	N—O^-
5	C(1)—S(1)	1.645(7)	C=S
	N(1)—O(1)	1.365(7)	N—O(H)
	N(2)—O(2)	1.307(7)	N^+—O^-
6	C(6)—S(3)	1.667(7)	C=S
	N(1)—O(1)	1.340(6)	N^+—O^-
	N(2)—O(2)	1.369(7)	N—O(H)
Average[a]	$C(sp^2)$—S(2)	1.751(17)	
	$C(sp^2)$=S(1)	1.671(24)	
	$N(sp^2)$—O(2)	1.396(12)	
	N^+—O^-	1.304(15)	

[a] Average bond distances taken from Ref. 14.

located in the vicinity of O(2). The structure was therefore modelled as containing an anionic component, $C_4H_4NOS_2^-$. In addition, the electron density around O(3) suggests the presence of four hydrogen atom sites; this was modelled as a disordered H_3O^+ unit with the three hydrogen atoms disordered equally over four sites. It should be noted that the location of hydrogen atoms, or the failure to locate them in this case, is not in itself sufficient evidence to deduce conclusively the presence of the anion. The small scattering power of hydrogen compared with the rest of the structure may not allow for the location of hydrogen atoms, even in low-temperature diffraction studies. Neutron diffraction experiments may allow for a more definite assignment. The ionic description proposed is, however, consistent with the observed thermal stability and solubility of **3** (discussed below).

The two independent HMTT molecules are linked directly through an O—H···O hydrogen bond [H(100)···O(2) = 1.62(2) Å] and also via the H_3O^+ ion [O(3)···O(2) = 2.752(4), H(3C)···O(2) = 1.85(4) Å; O(3)···S(1) = 3.407(4), H(3B)···S(1) = 2.50(3) Å]. These units are then linked through the H_3O^+ ion [O(3)···S(1) = 3.334(4), H(3D)···S(1) = 2.38(2) Å; O(3)···S(3) = 3.294(4), H(3A)···S(3) = 2.37(3) Å] to form centrosymmetric 'double chains' which run along the *b* direction [Fig. 1(b)].

Further characterization of 3

The hydrate **3** was isolated from the as-supplied sample of HMTT by separation of water-soluble and organic-soluble components. Compound **3** was present in the bulk only as a minor constituent (ca 5 mg in 1 g of HMTT), and additional peaks corresponding to **3** were not observable in the PXRD pattern of HMTT prior to separation. A sufficient quantity of **3** was isolated to permit collection of PXRD data and the pattern compares well with that simulated from the single-crystal structure (Fig. 2). The melting point of **3** is 126–128 °C, compared with 92–93 °C for the anhydrous **2**. PXRD performed at 100 °C showed that the hydrate structure remains unchanged at the elevated temperature. This enhanced thermal stability compared with **2** is consistent with the proposed ionic structure of the hydrate. In addition, **3** was observed to be highly soluble in water.

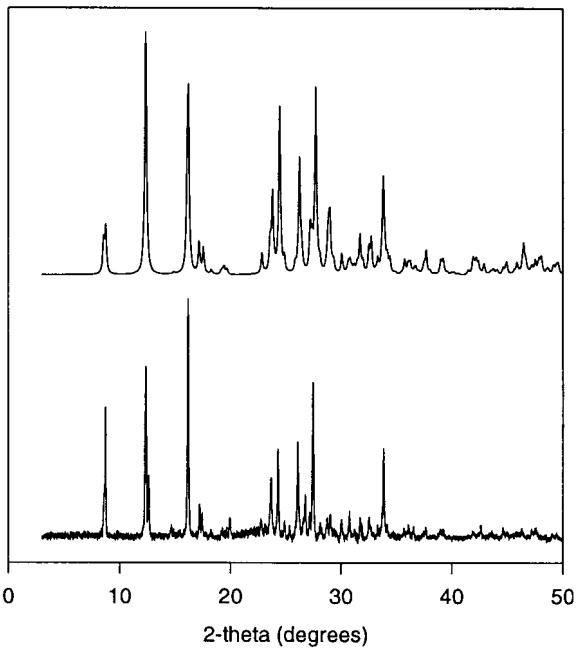

Figure 2. Simulated (top) and measured (bottom) PXRD patterns for the hydrate **3**

Crystal structure of 5

Recrystallization of HMTT from DMSO solution produced crystals of the oxidation product, 3-hydroxy-4-[3-oxo-4-methyl-2(3*H*)-thiazol-2-yl]thio-2(3*H*)-thiazolethione (**5**) [Fig. 3(a)]. The bond orders were assigned on the basis of the C—S and N—O bond distances (Table 1) and it was possible to locate H(100) in a difference Fourier map. In the solid state, the fixed C(2)—S(3)—C(5) unit enforces conformational chirality and both enantiomers are present in the crystal. H(100) is involved in an intermolecular hydrogen bond with O(2) [H(100)···O(2) = 1.71(3) Å], linking the molecules into helices running along the *c* direction [Fig. 3(b)]. Each helix contains alternate molecules of each enantiomer and adjacent helices have opposite handedness.

Crystal structure of the mixed crystal 6

Co-crystallization of **1** and **2** from DMSO solution

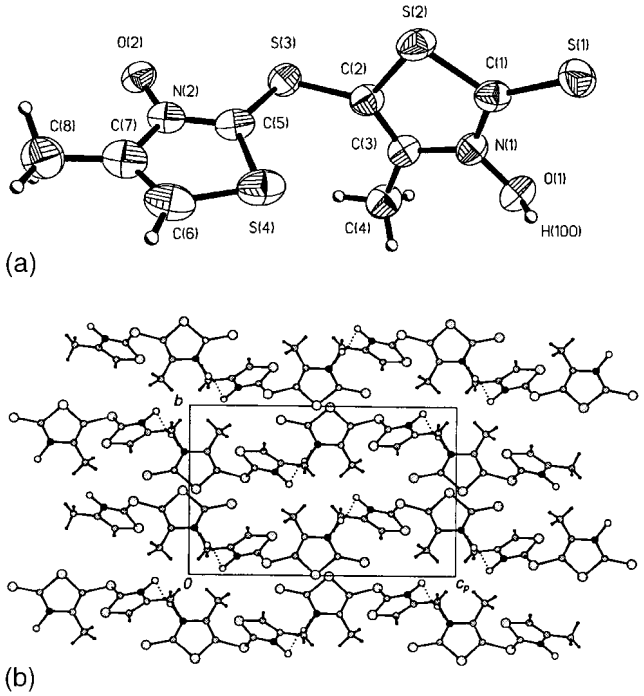

Figure 3. (a) Molecular unit in **5** showing displacement ellipsoids at 50% probability. (b) View of **5** along the *a* direction, showing antiparallel helical chains running along the *c* direction

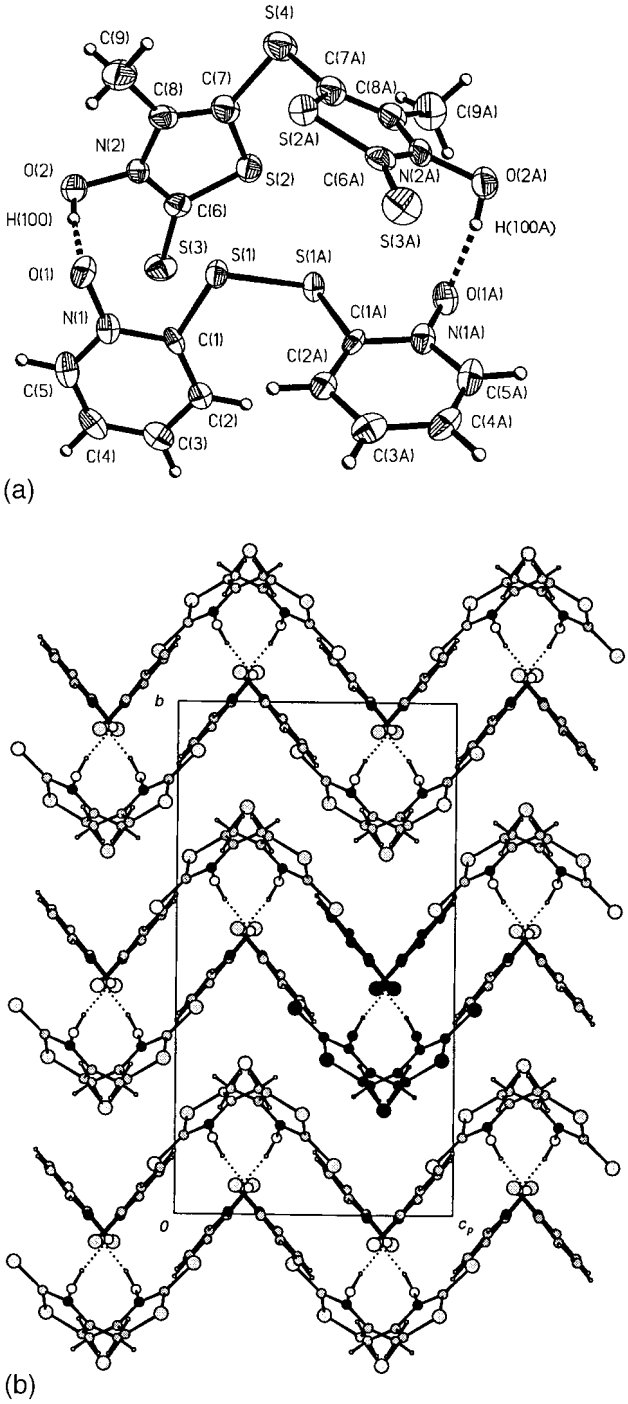

Figure 4. (a) Molecular units in the solid-state structure of **6** with displacement ellipsoids at 50% probability. O—H···O hydrogen bonds are indicated by dotted lines. A twofold rotation axis passes through S(4) and the midway point of the S(1)—S(1A) bond. Symmetry equivalent atoms are denoted by the suffix A. (b) View of **6** along the *a* direction showing the hydrogen-bonded dimers linked into crinkled sheets. A single discrete dimer is shaded grey

produced single crystals of **6** containing both DTPO and 5,5′-thiobis[3-hydroxy-4-methyl-2(3*H*)-thiazolethione], denoted THMTT, a new molecule derived from **2** [Fig. 4(a)]. In the THMTT molecule, the C—S and N—O bond distances are suggestive of the thione tautomer (Table 1) and it was possible to locate H(100) in a difference Fourier map. The DTPO and THMTT molecules are linked into pairs via O—H···O interactions [H(100)···O(1) = 1.71(3) Å]. The relatively large N(1)—O(1) bond distance (compared with the average value and the value for the N^+—O^- unit in **5**) may result from the involvement of O(1) in this interaction. A twofold rotation axis parallel to *b* passes through S(4), relating the two crystallographically unique halves of each molecule. The DTPO–THMTT pairs are linked via C—H···O interactions [H(4)···O(2) = 2.51 Å] into crinkled sheets parallel to the (101) plane [Fig. 4(b)].

DISCUSSION

Crystal structures and physico-chemical properties of 1, 2 and 3

The crystal structure of **1** has been reported previously.[10,11] Compound **1** exists exclusively as the thione tautomer in the solid state and the hydrogen atom of the hydroxyl group, H(100), is involved in an intramolecular hydrogen bond with the sulfur atom of the thione group. As a result, the predominant intermolecular interactions within **1** are weak C—H···O hydrogen bonds, linking the

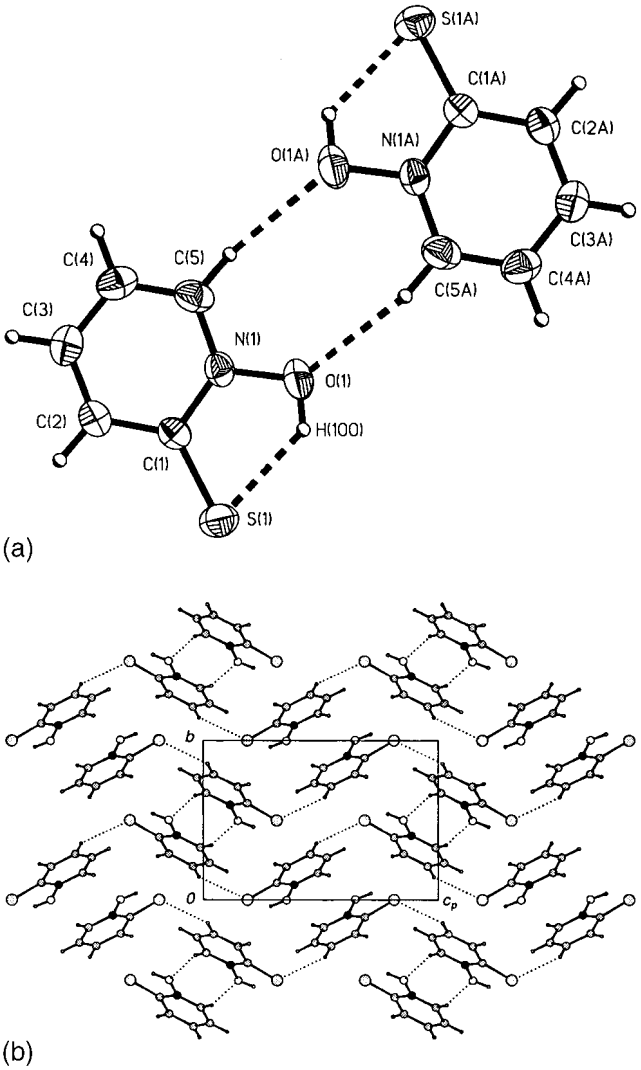

Figure 5. (a) Centrosymmetric dimer observed in the structure of pyrithione (**1**). Intramolecular O—H···S and intermolecular C—H···O interactions are indicated by dotted lines. Symmetry-equivalent atoms are denoted by the suffix A. (b) View of **1** along the *a* direction showing the centrosymmetric dimers packed in a herringbone manner. Short intermolecular C—H···S contacts are indicated by dotted lines. Intramolecular hydrogen bonds are omitted

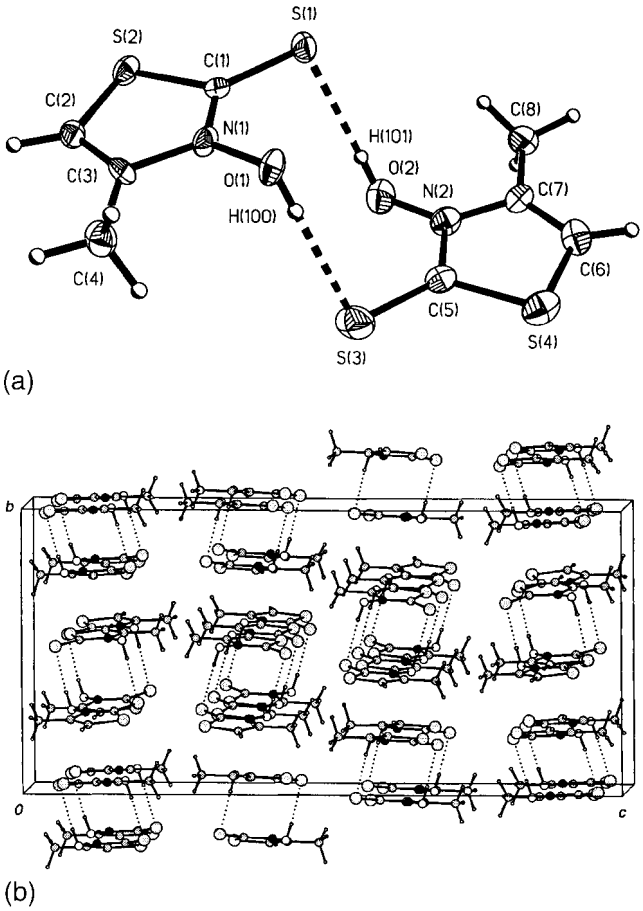

Figure 6. (a) Pseudo-centrosymmetric dimer unit observed in the solid-state structure of **2**. O—H···S interactions are indicated by dotted lines. (b) View of **2** showing the centrosymmetric dimers linked into chains by C—H···O interactions

molecules into centrosymmetric dimers [Fig. 5(a)] which pack in a herringbone arrangement [Fig. 5(b)]. Short S···H contacts within the structure also suggest weak C—H···S interactions.

Determination of the crystal structure of **2** was complicated by difficulty in obtaining single crystals of sufficient size for x-ray diffraction analysis. The structure has been solved by combination of a single-crystal study employing synchrotron radiation and powder x-ray diffraction analysis (A. D. Bond, N. Feeder, S. J. Teat and W. Jones, Tetrahedron submitted for publication). Two independent molecules are present in the asymmetric unit. The intramolecular hydrogen bond observed in **1** is not present in **2** since the geometry of the five-membered thiazole ring results in an O···S distance and O—H···S angle unsuitable for such an interaction. Thus, the hydrogen atoms of the hydroxyl groups, H(100) and H(101), are available for intermolecular hydrogen bonding and O—H···S interactions link the molecules into pseudo-centrosymmetric dimers [Fig. 6(a)]. The pseudo-centres of symmetry in the dimeric units do not coincide with crystallographic centres of symmetry. C—H···O interactions link the dimer units into chains running parallel to the *a* direction [Fig. 6(b)].

Selected physico-chemical properties of **1** and **2** may be related to their solid-state structures by consideration of the intermolecular interactions within the crystals. For example, the materials melt at a temperature where the entropy gain from randomising the molecular orientations in the liquid state (ΔS_{fus}) overcomes the enthalpy loss due to breaking the intermolecular interactions in the solid state (ΔH_{fus}). It is not possible to extract a value for ΔH_{fus} directly from the calculated lattice energy, since this encompasses both fusion and vaporisation terms

(ΔH_{vap}). It is likely, however, that ΔH_{vap} will be similar for similar organic molecules, so that the relative magnitudes of E_{latt} give a good indication of the relative magnitudes of ΔH_{fus}. [There is some confusion with regard to the sign of E_{latt}. In many physical chemistry texts, lattice enthalpy is described as 'the standard enthalpy change accompanying the formation of a gas of ions/molecules from a crystalline solid.'[15] Such a definition clearly necessitates an endothermic term. In other texts, the opposite definition is employed, giving an exothermic term. The trend in the literature is towards the exothermic definition and this convention is adopted here. Thus, lattice enthalpy is the negative of sublimation enthalpy and the absolute value must be used in relation to the (always endothermic) enthalpy of fusion. It should also be noted that values of E_{latt} calculated via molecular mechanics methods refer to those at absolute zero. At real temperatures, the lattice enthalpy is related to the lattice energy by the expression $H_{latt} = E_{latt} + nRT$ (assuming ideal behaviour in the gaseous state). For conformationally flexible molecules, an additional enthalpy term may arise from a conformational change of the molecule between the solid and gas phases; this also is not accounted for in the molecular mechanics method. In general, absolute values calculated for E_{latt} are not reliable, but it is clear that relative values give a good guide to the relative stabilities of organic solids.] Thus, the thermal stabilities of **1** and **2** may be rationalized by consideration of their calculated lattice energies. The calculated lattice energy in **1** is $-83.0\ kJ\ mol^{-1}$, corresponding to a melting point of 69–72 °C, while in **2** the calculated lattice energy is $-95.5\ kJ\ mol^{-1}$, giving a correspondingly higher melting point of 92–93 °C.

The solubility of an organic material is similarly governed by the relative strengths of the intermolecular forces in the solid and in solution, i.e. the interactions between solid and solvent molecules must be sufficient to overcome the interactions holding together the solid and those holding together the solvent. More precisely, for dissolution to occur spontaneously, the free energy released on dissolution must exceed the lattice free energy of the solid plus the free energy required to disrupt the liquid solvent. For similar organic molecules dissolving in the same solvent, the free energy terms (encompassing both enthalpy and entropy) arising from solvent disruption will be similar, and the entropy terms arising from dissolution of the solids will be similar. Thus, the relative solubilities of the two materials are related qualitatively to the enthalpy terms involved with disrupting the solid. This may be expressed quantitatively as the ideal law of solubility:

$$\ln x = \frac{-\Delta H_{fus}}{R}\left(\frac{1}{T} - \frac{1}{T^*}\right)$$

where x is the mole fraction of the solute at temperature T and T^* is the melting point of the pure solute.[16] Taking again the relative values of E_{latt} as a qualitative guide to the relative values of ΔH_{fus}, it may be predicted that organic materials with larger calculated lattice energies (more stable) and higher melting points will exhibit lower solubilities at normal temperatures. In this case, the solubility of **1** in a given solvent would be expected to exceed that of **2**. Solubility measurements in water at 20 °C give values of ca 2.5 g dm^{-3} for **1** and 2.1 g dm^{-3} for **2**.

The crystal structure of the hydrate **3** contains an extensive network of strong O—H···O hydrogen bonds, giving rise to a large lattice energy and significant thermal stability. This is confirmed by the elevated melting point of **3** compared with **2** and the observation that the structure remains unchanged at 100 °C (above the melting point of the anhydrous material **2**). The enhanced solubility of **3** in water suggests an ionic structure, consistent with the x-ray analysis. Here, the strong interactions between the ionic components and the solvent greatly increase the enthalpy of solvation for **3** and solubility predictions based upon comparisons with the lattice energies of **1** and **2** are not valid—the system in this case is far from obeying the ideal law of solubility.

Crystal structures and host–guest chemistry of 4, 5 and 6

The crystal structure of **4** has been determined previously.[12] The DTPO molecules associate via C—H···O interactions to form two interpenetrated homochiral networks (Fig. 7). Each molecule makes eight C—H···O contacts, six to molecules within the same homochiral network and two to molecules from the other network. Similar comparisons based upon the calculated lattice energies are possible for the melting points of **4** and **5**. Compound **4** has a calculated lattice energy of $-158.9\ kJ\ mol^{-1}$ and a melting point of 176–178 °C (the melting point of DTPO has been reported previously as 205 °C;[12] we determined the melting point using single

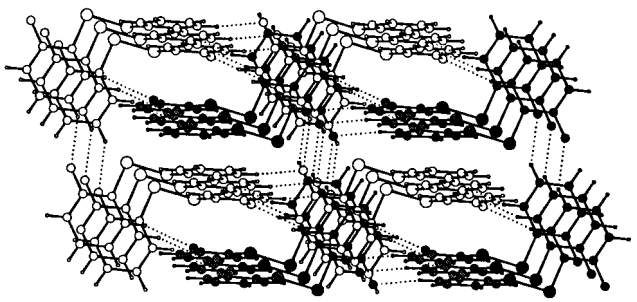

Figure 7. Solid-state structure of DTPO (**4**), showing interpenetrated homochiral networks shaded white and grey. C—H···O interactions are indicated by dotted lines

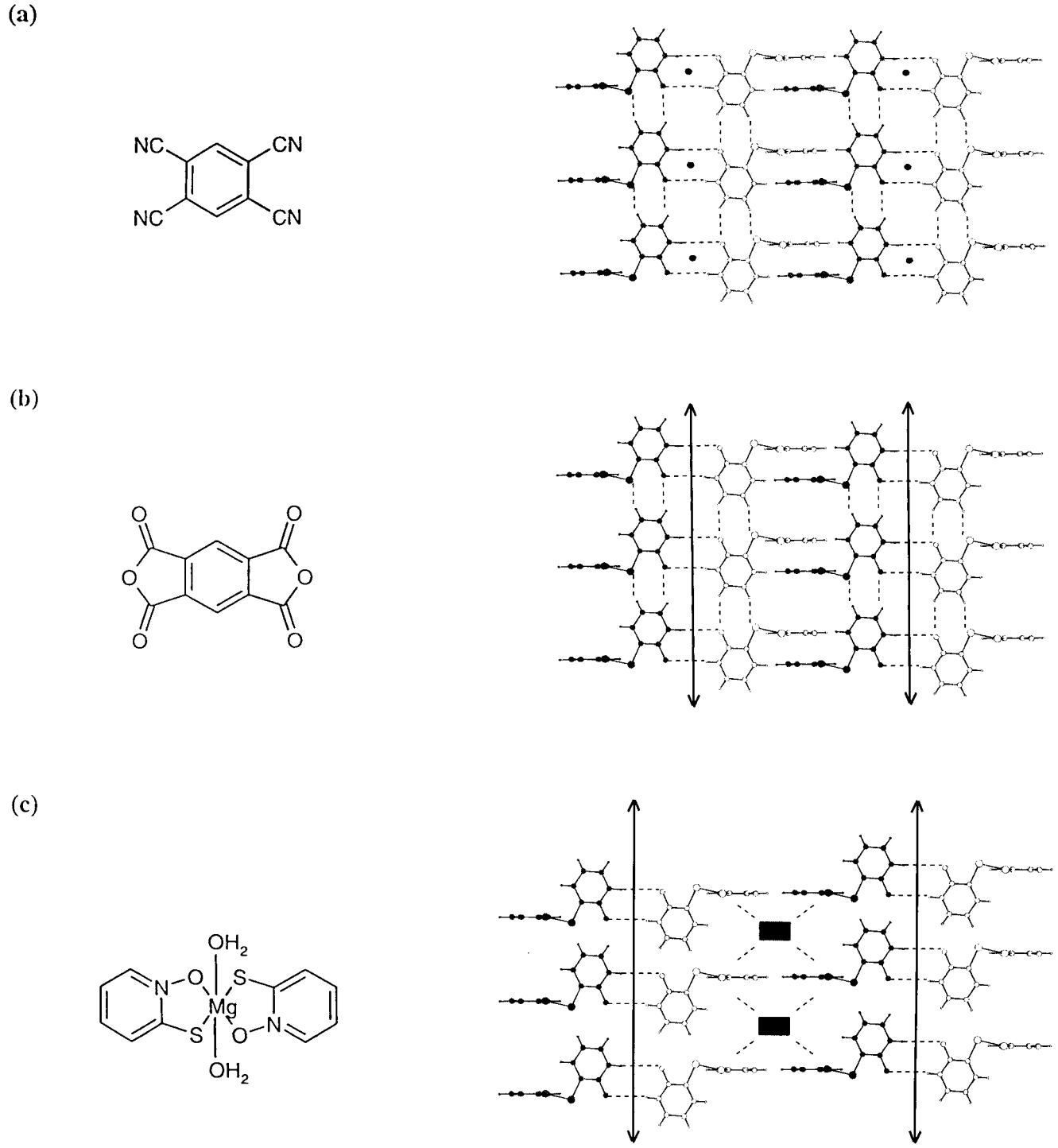

Scheme 1. Schematic representations of the structures of (a) $[DTPO]_2[TCNB](H_2O)_4$, isolated molecules: zero-dimensional insertion; (b) $[DTPO]_2[PMDA]$, chains running in direction of arrows: one-dimensional insertion and (c) $[DTPO]_2[Mg(C_5H_4NOS)_2(H_2O)_2]$, chains running in direction of arrows and out of plane of paper (denoted by ■): two dimensional insertion

crystals from several different batches and consistently obtained the value indicated), whereas **5**, which contains stronger O—H···O interactions, has a calculated lattice energy of -167.2 kJ mol^{-1} and a correspondingly higher melting point of 200–202 °C.

The open-network structure of DTPO has been shown previously to be suitable for guest insertion. Host–guest complexes of DTPO have been reported with tetracyanobenzene (TCNB),[12] pyromellitic dianhydride (PMDA)[12] and a diaquamagnesium complex of pyrithione, $Mg(C_5H_4NOS)_2(H_2O)_2$.[13] Comparison of the three structures suggests that the nature of the guest

insertion may be related to the spatial distribution of the supramolecular functionality of the guest (Scheme 1). In $[DTPO]_2[TCNB](H_2O)_4$, the guest molecules contain no supramolecular functionality and they are incorporated as isolated molecules. This may be termed a 'zero-dimensional' insertion. In $[DTPO]_2[PMDA]$, the PMDA molecules are able to associate via C—H···O interactions to yield one-dimensional chains which thread the DTPO lattice in a single direction, i.e. a one-dimensional insertion. The DTPO molecules remain bound via C—H···O interactions to yield a solid-state polypseudorotaxane structure. In $[DTPO][Mg(C_5H_4NOS)_2(H_2O)_2]$, $Mg(C_5H_4NOS)_2(H_2O)_2$ molecules are able to form similar chains through C—H···S interactions. The presence of additional water molecules above and below the plane of the $[Mg(C_5H_4NOS)_2(H_2O)_2]_n$ chains facilitates additional interactions with the DTPO lattice and give rise to insertion in two perpendicular directions, i.e. a two-dimensional insertion.

In the case of **6**, however, the formation of strong O—H···O bonds with the THMTT molecule results in complete disruption of the C—H···O bonded network of the DTPO lattice. This special case arises because the DTPO and THMTT molecules show complete supramolecular complementarity, i.e. the geometries of the two components are exactly suited for forming discrete hydrogen-bonded dimers.

CONCLUSIONS

Determination of the crystal structures of organic materials is essential for the rationalization of their physico-chemical properties. An illustration of the importance of solid-state studies is given in this case by the identification of the hydrate **3** within the bulk sample of **2**. If **2** were to be applied as a pharmaceutical product, for example, its equilibrium solubility would be used to determine its dosage. Failure to account for the additional phase, with solubility orders of magnitude greater than that of **2**, may have serious consequences. Consideration of intermolecular interactions within the solid state can give an insight into relevant physico-chemical properties. The calculated lattice energy, readily available from molecular mechanics methods, provides a quantitative measure of the intermolecular forces and can be employed in a predictive sense. Predictions are necessarily qualitative, but may provide a useful guide to the relative thermal stabilities or solubilities of organic solids.

EXPERIMENTAL

Preparation of the materials. 1-Hydroxy-2(1*H*)-pyridinethione and 3-hydroxy-4-methyl-2(3*H*)-thiazolethione were obtained from Aldrich Chemical Company. The bulk sample of HMTT was found to contain both the anhydrous material (**2**) and the hydrate (**3**); on dissolution in dichloromethane (DCM), a small amount of **3** remained undissolved, from which a single crystal was selected and used for x-ray analysis. Compounds **4** and **5** were prepared by recrystallization of **1** and **2**, respectively, from dimethyl sulfoxide (DMSO) solution in air.

Table 2. Crystallographic data for **3, 5** and **6**

	3	**5**	**6**
Empirical formula	$C_8H_{12}N_2O_3S_4$	$C_8H_8N_2O_2S_4$	$C_{18}H_{16}N_4O_4S_7$
M(g mol^{-1})	312.44	292.40	576.76
T(K)	180(2)	296(2)	210(2)
Crystal system	Monoclinic	Monoclinic	Monoclinic
Space group	$P2_1/n$	$P2_1/c$	$C2/c$
Crystal size (mm)	0.18 × 0.07 × 0.05	0.50 × 0.40 × 0.10	0.15 × 0.15 × 0.10
Radiation [λ (Å)]	Mo Kα (0.7107)	Cu Kα (1.5418)	Cu Kα (1.5418)
a(Å)	14.326(3)	7.6294(15)	10.264(2)
b(Å)	6.5120(10)	10.006(2)	20.377(4)
c(Å)	14.578(3)	15.727(3)	11.141(2)
α(°)	90	90	90
β(°)	91.26(3)	90.57(3)	95.56(3)
γ(°)	90	90	90
V(Å^3)	1359.7(5)	1200.6(4)	2319.2(8)
Z	4	4	4
μ(mm^{-1})	0.696	7.183	6.610
Reflections collected	7013	1686	1947
Unique reflections	3077	1510	1440
R_{int}	0.072	0.074	0.041
$\Delta\rho_{max}$, $\Delta\rho_{min}$ (e Å^{-3})	0.562, −0.575	0.413, −0.885	0.669, −0.585
$R1$ [$I > 2\sigma(I)$]	0.062	0.076	0.057
$wR2$ [$I > 2\sigma(I)$]	0.159	0.219	0.138
S	1.073	1.066	1.043

Compound **6** was prepared from a 1:2 mixture of **1** and **2** in DMSO solution. For both **5** and **6** the products were isolated as single crystals, with insufficient material for PXRD analysis.

Determination of melting points and solubilities. Melting points were obtained from single crystals by use of an optical microscope with hot-stage attachment. Solubilities were measured by suspending a known mass in water, sonicating for 5 min and separating the undissolved solid by centrifugation.

Single-crystal x-ray diffraction. For **3**, data were collected on a Nonius Kappa CCD area-detector diffractometer using Mo Kα radiation. Lattice parameters were determined from 10 images recorded with 1° φ scans and subsequently refined on all data. A 180° φ range was scanned with 2° steps during data collection with an exposure time of 20 s per frame and the crystal-to-detector distance fixed at 35 mm. The data were processed using the HKL package.[17] An absorption correction was not applied since $\mu^* r < 0.1$.[18]

Data were collected for **5** and **6** on a Stoe STADI four-circle diffractometer using Cu Kα radiation. Cell parameters were determined from 25 well-centred reflections in the range $40 < \theta < 50°$. An absorption correction was applied using ψ scans,[19] and data reduction was carried out using the REDU4 package.[20] In all cases, the structures were solved by direct methods using SHELXS-97[21] and refined on F^2 using SHELXL-97.[22] Hydrogen atoms were placed geometrically on the aromatic rings and methyl groups and refined using a riding model. Hydrogens on the hydroxyl groups were located in difference Fourier maps and refined with a fixed isotropic displacement parameter (0.05 Å^2) and the O—H bond distance restrained to be 0.82(2) Å (O—H distance of 0.82 Å derived from SHELXL default[23]). The crystallographic data are summarized in Table 2.

Variable-temperature powder x-ray diffraction (PXRD). Variable-temperature PXRD analysis was carried out with Ge(111)-monochromated Cu Kα radiation (λ = 1.5406 Å) using a Stoe STADI-P high-resolution diffractometer equipped with a furnace attachment and a position-sensitive detector (PSD) covering ca 6° in 2θ. Samples were loaded in 0.5 mm glass capillaries and heated *in situ* with the capillary open to the atmosphere. The pattern was measured over the range $3 \leq 2\theta \leq 50°$ with a step size of 2.5° and a count time of 360 s per step.

Lattice energy calculations. Lattice energy calculations were performed within the Cerius^2 molecular modelling environment.[24] Electrostatic potential derived charges were calculated using the MOPAC (AM1) semi-empirical molecular orbital program and the Dreiding force field with default parameters was employed.[25] To assess the suitability of the force field, energy minimization was carried out for **1** and **2**, initially with rigid-body rotations and translations within a fixed unit cell and then with unit-cell parameters also relaxed (within the symmetry constraints of the crystal system). The final minimized model for **1** had unit-cell parameters a = 5.833, b = 7.668, c = 12.167 Å, β = 94.39°, and for **2**, a = 6.472, b = 13.559, c = 28.458 Å. The small differences between the observed and minimized unit-cell parameters (mean change in cell length 0.388 Å for **1** and 0.234 Å for **2**) indicate that the force field provides an adequate description of the intermolecular interactions.

EPOC material

The crystal structures of **1–6** and the host–guest complexes referred to in the Discussion section are available in downloadable CIF or PDB format at the epoc website at http://www.wiley.com/epoc.

Acknowledgements

We are grateful to the EPSRC and Avecia Limited for funding via a CASE award to A.D.B., and to Drs Neil Feeder and John Davies for assistance with the single-crystal x-ray diffraction analyses.

REFERENCES

1. Jones W (ed). *Organic Molecular Solids: Properties and Applications*. CRC Press: New York, 1997.
2. Gavezzotti A, Filippini G. *J. Am. Chem. Soc.* 1995; **117**: 12299–12305.
3. Haleblian J, McCrone W. *J. Pharm. Sci.* 1969; **58**: 911–929.
4. Khankari RK, Grant DJW. *Thermochim. Acta* 1995; **248**: 61–79.
5. Theocharis CR, Desiraju GR, Jones W. *J. Am. Chem. Soc.* 1984; **106**: 3606–3609.
6. Paulus W. *Microbicides for the Protection of Materials: a Handbook*. Chapman and Hall: London, 1993; 294–303.
7. Albert A. *Selective Toxicity: the Physicochemical Basis of Therapy*. Chapman and Hall: London, 1973; 378.
8. Beckwith AJJ, Hay BP. *J. Am. Chem. Soc.* 1988; **110**: 4415–4416.
9. Hartung J, Schwarz M. *Synlett* 1997; 848–850; 1116.
10. Hartung J, Kneuer R, Schwarz M, Svoboda I, Feuss H. *Eur. J. Org. Chem.* 1999; 97–106.
11. Bond AD, Jones W. *Acta Crystallogr., Sect. C* 1999; **55**: 1536–1538.
12. Bodige SG, Rogers RD, Blackstock SC. *J. Chem. Soc., Chem. Commun.* 1997; 1669–1670.
13. Bond AD, Jones W. *Acta Crystallogr., Sect. C* 2000; **56**: 436–437.
14. Allen FH, Kennard O, Watson DG, Brammer L, Orpen AG, Taylor R. *J. Chem. Soc., Perkin Trans. 2* 1987; S1–S18.
15. Atkins PW. *Physical Chemistry* (4th edn). Oxford University Press: Oxford, 1990; 49.
16. Atkins PW. *Physical Chemistry* (4th edn). Oxford University Press: Oxford, 1990; 170.
17. HKL Data Processing System (Version 1.11). Nonius: Delft, 1998.
18. Notes for Authors, *Acta Crystallogr., Sect. C* 2000; **56**: 125–132.
19. North ACT, Phillips DC, Mathews FS. *Acta Crystallogr., Sect. A* 1968; **24**: 351–359.

20. REDU4 Program for Data Reduction (version 7.03). Stoe: Darmstadt, 1992.
21. Sheldrick GM. SHELXS-97 Program for Crystal Structure Solution. University of Göttingen: Göttingen, 1997.
22. Sheldrick GM. SHELXL-97 Program for Crystal Structure Refinement. University of Göttingen: Göttingen, 1997.
23. Sheldrick, GM. SHELXL-97 Manual. University of Göttingen: Göttingen, 1997.
24. *Cerius*^{2} (Version 4.0) Molecular Modelling Package. Molecular Simulations: San Diego, CA, 1999.
25. Mayo SL, Olafson BD, Goddard WA. *J. Phys. Chem.* 1990; **94**: 8897–8909.